

Chemical Science

Accepted Manuscript

This article can be cited before page numbers have been issued, to do this please use: J. Ming, J. Zhang, Y. Hu, K. Lan, D. Zhang, P. Li, J. Miao, J. Jiang, X. Zhang, H. Zhong, P. Yu and C. Cheng, *Chem. Sci.*, 2026, DOI: 10.1039/D6SC01132B.



This is an Accepted Manuscript, which has been through the Royal Society of Chemistry peer review process and has been accepted for publication.

Accepted Manuscripts are published online shortly after acceptance, before technical editing, formatting and proof reading. Using this free service, authors can make their results available to the community, in citable form, before we publish the edited article. We will replace this Accepted Manuscript with the edited and formatted Advance Article as soon as it is available.

You can find more information about Accepted Manuscripts in the [Information for Authors](#).

Please note that technical editing may introduce minor changes to the text and/or graphics, which may alter content. The journal's standard [Terms & Conditions](#) and the [Ethical guidelines](#) still apply. In no event shall the Royal Society of Chemistry be held responsible for any errors or omissions in this Accepted Manuscript or any consequences arising from the use of any information it contains.

ARTICLE

A Dual-Responsive Cationic Acridinium Nanochoop: Redox Activity and Acid/Base-Controlled Reversible Guest Capture and Release

Jiao Ming^a, Jin Zhang^b, Yan Hu^a, Kai Lan^a, Dongmei Zhang^a, Ping Li^a, Jiarong Miao^a, Jiyong Jiang^a, Xiaobo Zhang^a, Hanchi Zhong^a, Peiyuan Yu^{*b} and Chuyang Cheng^{*a}

Received 00th January 20xx,
Accepted 00th January 20xx

DOI: 10.1039/x0xx00000x

In this work, we report a fully conjugated, radially cationic nitrogen-doped cycloparaphenylene derivative, **Ad[10]CPP⁺**, constructed using the acridinium moiety as a functional building block. This compound exhibits remarkable reversibility in structural transformations under chemical stimuli and tunable redox behavior under electrochemical stimuli. Cyclic voltammetry reveals that **Ad[10]CPP⁺** possesses multiple oxidation states and demonstrates significant redox versatility. Furthermore, **Ad[10]CPP⁺** can reversibly transform from a near-circular configuration to a water-droplet shape upon hydroxide attack on the acridinium moiety when the acid concentration is lowered. The host-guest interaction between fullerene (C₆₀) and **Ad[10]CPP⁺** was confirmed by NMR spectroscopy and single-crystal X-ray diffraction. Significantly, the host-guest system exhibits excellent fatigue resistance, enabling at least five consecutive cycles of chemically triggered fullerene capture and release through reversible structural transformations.

Introduction

Cycloparaphenylenes (CPPs), aromatic macrocycles comprised of *para*-phenylene units, have garnered considerable attention since their first synthesis^[1-8]. The interest is primarily attributed to their inherent ring strain^[9-15] and unique radial cyclic π -conjugated architectures^[16-21]. Over the past decade, the field has witnessed remarkable progress, as evidenced by the successful synthesis of CPPs and their derivatives of varying sizes^[22-28]. Despite these advancements, the incorporation of heteroatoms, particularly nitrogen, remains underexplored^[8]. Replacing phenylene units with nitrogen-containing aromatic rings can endow CPPs with acid-base responsiveness^[29], metal coordination capabilities^[30], and synthetic handles for constructing mechanically interlocked molecules^[31-33]. Subsequent alkylation of these nitrogen atoms can convert the neutral macrocycles into cationic ones, introducing redox activity^[34, 35]. Both the amount and position of nitrogen doping can effectively modulate the photophysical^[36] and supramolecular properties of CPPs^[37]. Notably, in most reported cases, nitrogen atoms are incorporated at lateral positions of the CPP skeleton (scheme 1a, left), as this approach aligns with conventional synthetic routes. In contrast, the direct fusion of nitrogen at the phenylene linkage sites, namely, axial doping, is far less common^[38-42]. Such a configuration is predicted to markedly influence the nanoring's photophysical profile, introduce multiple accessible redox states^[38], and

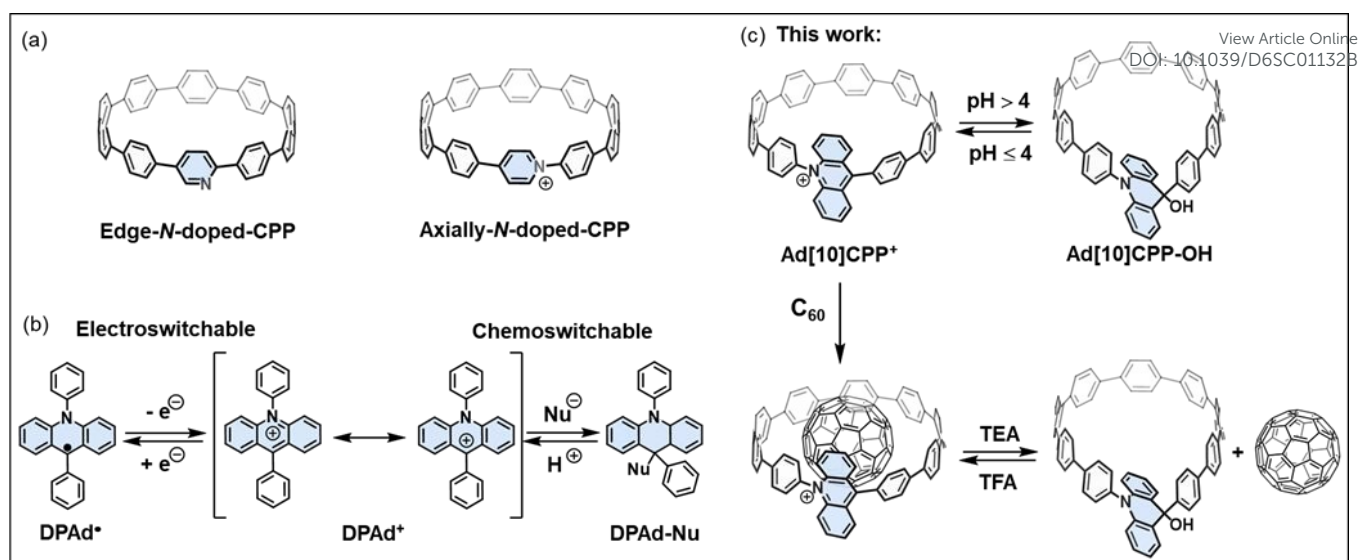
create a cavity with tunable size^[39]. However, the limited examples of axially *N*-doped carbon nanorings reported to date are, strictly speaking, not fully conjugated CPPs. Recently, we reported the first fully conjugated cationic CPPs bearing pyridinium units at the phenylene linkages^[43] (Scheme 1a, right), a long-standing synthetic challenge due to ring strain and cation instability under basic conditions. This synthetic challenge was effectively overcome by introducing *N*-phenylpiperidine derivative strain-release unit followed by aromatization to construct pyridinium moiety. In the present work, we extend this design by employing π -expanded motif, in the form of an acridine fragment, as a strain-release unit. This approach not only enhances synthetic accessibility but also unlocks distinct functional advances. Specifically, we demonstrate that installing cationic nitrogen at the phenylene linkage sites in the form of acridinium enables reversible, stimuli-responsive switching of the macrocyclic framework between configurations in response to electrochemical and acid–base stimuli. This structural dynamism, in turn, facilitates controlled capture and release of guest molecules, advancing CPPs toward adaptive host–guest systems.

The rigid and curved conjugated structure of CPPs serves as ideal host molecules for fullerenes^[44-50]. Their complementary shape and size facilitate strong π - π interactions with fullerenes, achieving binding constants of $10^5 \sim 10^6$ M⁻¹. The rigid and strained macrocyclic constitution, however, also poses a challenge for incorporating reversible guest capture and release functionality. Introducing stimuli-responsive motifs that can reversibly modulate the strained framework offers an effective

^a Key Laboratory of Green Chemistry & Technology, University of Sichuan, Chengdu, 610064, China. E-mail: cycheng@scu.edu.cn

^b Department of Chemistry and Guangming Advanced Research Institute, Southern University of Science and Technology, Shenzhen, 518055, China. E-mail: yupy@sustech.edu.cn





Scheme 1. Design concept of an acridinium functionalized cycloparaphenylene.

strategy for achieving controlled guest capture and release. While several studies have incorporated stimuli-responsive motifs into CPPs to modulate the geometry of the strained macrocycle^[16, 51-54], to the best of our knowledge, no examples of stimuli-responsive guest capture and release for CPPs have been reported thus far.

The acridinium unit is known for its reversible structural transformation in response to electrochemical and chemical stimuli^[55-63]. Specifically, 9,10-diphenylacridinium (**DPAd**⁺) is highly susceptible to nucleophilic attack and can reversibly transition between its radical state and cationic form under electrochemical control (scheme 1b). In this study, we incorporate **DPAd**⁺ fragment into the CPP skeleton to construct a functionalized strain macrocycle similar in size to [10]CPP, namely, **Ad[10]CPP**⁺ (scheme 1c). We carried out a comprehensive investigation into the synthesis, as well as structural, optical, electronic, and computational properties of **Ad[10]CPP**⁺. Our findings revealed that **Ad[10]CPP**⁺ undergoes reversible structural transformations under electrochemical and acid/base stimulation. Furthermore, we performed extensive studies on the host-guest chemistry of **Ad[10]CPP**⁺ and successfully obtained the solid-state suprastructure of C_{60} captured by **Ad[10]CPP**⁺. Most notably, **Ad[10]CPP**⁺ demonstrated the ability to bind and release C_{60} in response to acid/base stimuli, exhibiting excellent fatigue resistance over multiple cycles. This approach offers significant potential for expanding the applications of CPPs in supramolecular chemistry and materials science.

Results and Discussion

Synthesis and structure characterization

The synthesis of the target molecule commenced with a macrocyclization step through a double-site Suzuki-Miyaura cross-coupling reaction between the bent dibromoacridine derivative **3** and the C-shaped diboronate^[15, 64] **7** (Figure 1a). Our initial strategy anticipated that the SnCl_2 -mediated

reductive aromatization^[65] would yield the desired acridinium product. However, the compound obtained did not align with our expectations; the ¹H NMR spectrum exhibited an unanticipated signal at 5.32 ppm, devoid of the characteristic deshielded aromatic signals above 8 ppm (Figure 2a, Figure S8). Moreover, the mass spectrometry data deviated by approximately one unit (Figure S21). Single-crystal X-ray diffraction analysis ultimately confirmed that the product was a macrocycle with the acridinium unit hydrogenated (**Ad[10]CPP-H**), featuring an sp^3 -hybridized carbon within the acridine moiety, which imparted a teardrop shape to the macrocycle with dimensions of 16.7 Å along the long axis and 11.0 Å along the short axis (Figure 1b). The over-reduction, while not the desired outcome, was not detrimental, as the product remained a macrocycle with a structure closely resembling our target. Subsequently, we endeavored to oxidize **Ad[10]CPP-H** using 2,3-dichloro-5,6-dicyano-1,4-benzoquinone (DDQ) to achieve the acridinium macrocycle. Despite our efforts, the product again closely resembled the expected macrocycle but exhibited an additional signal at 2.86 ppm in ¹H NMR spectrum, with the mass data offset by around 17 units (Figure 2b, Figure S11, S22). Single-crystal X-ray diffraction revealed a macrocycle of similar teardrop shape (**Ad[10]CPP-OH**), with the only difference being the oxidation of a C-H bond to a C-OH group compared with **Ad[10]CPP-H** (Figure 1c).

With the macrocycle in the anticipated oxidative state, we proceeded to acidify the sample using HBF_4 to protonate the hydroxy group and induce dehydration, aiming to convert the macrocycle into the cationic acridinium-functionalized final product (**Ad[10]CPP•BF₄**). The ¹H NMR spectrum demonstrated a complete transformation from **Ad[10]CPP-OH** to a new species, with the characteristic deshielded aromatic signal for H_a at 8.30 ppm and H_c at 7.99 ppm (Figure 2c and Figure S15). The high resolution MALDI-TOF MS spectrum confirmed the expected molecular weight of the acridinium macrocyclic cation (Figure S23), thereby validating the successful synthesis of the desired macrocycle. **Ad[10]CPP•TFA** is also obtained by treating



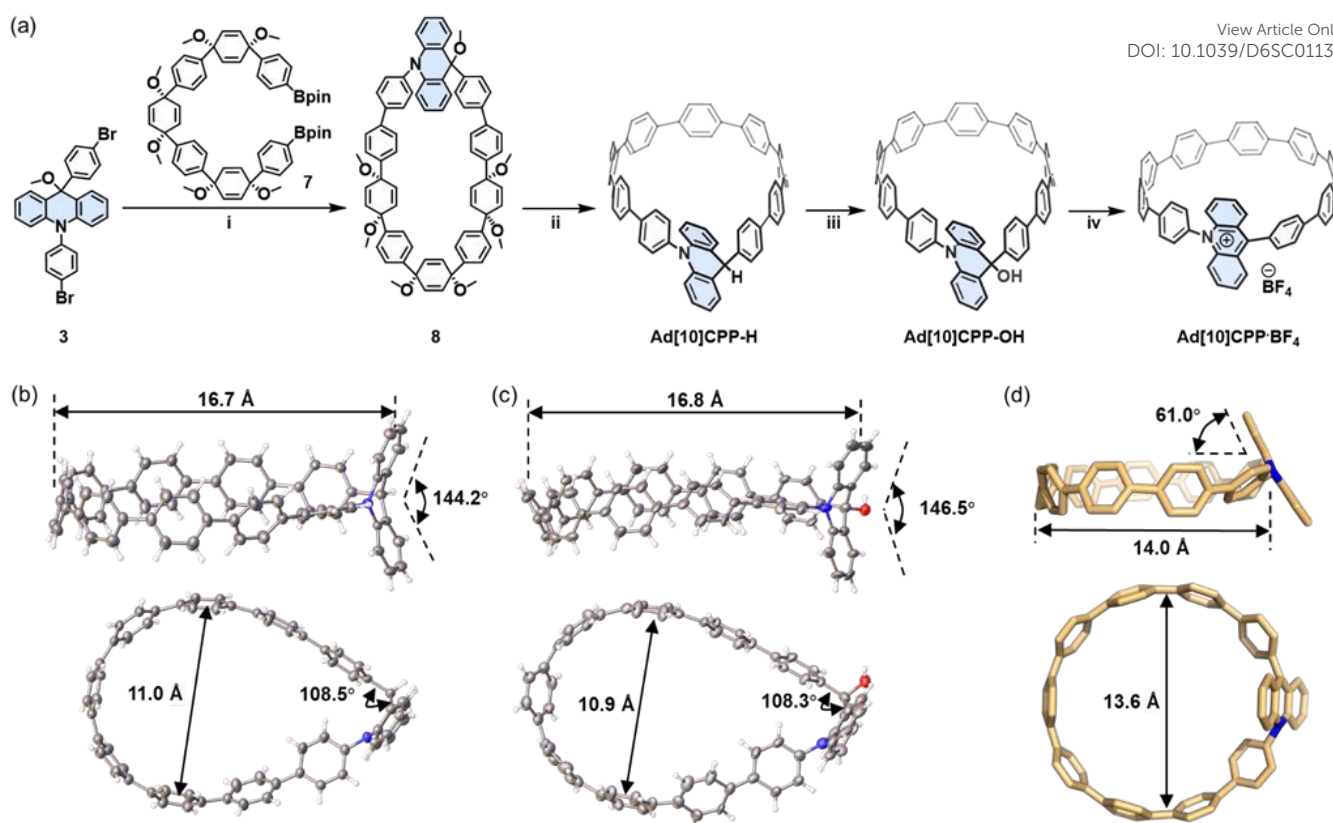


Figure 1. (a) The synthetic route of Ad[10]CPP•BF₄. Reaction conditions: (i) Pd(PPh₃)₄, NaHCO₃, n-Bu₄NBr, toluene/methanol/H₂O, 90 °C, 24 h. (ii) SnCl₂·2H₂O, concentrated HCl, THF, rt, 12 h, 13% over two steps. (iii) DDQ, CH₂Cl₂, rt, 12 h, 54%. (iv) HBF₄ (40% aq), CH₂Cl₂, rt, 3h, quantitative by NMR. The ORTEP drawing of X-ray solid-state structure of (b) Ad[10]CPP-H and (c) Ad[10]CPP-OH. Thermal ellipsoids are set at 30 % probability. Grey C, White H, Blue N, Red O. Solvent molecules are omitted for clarity. For crystallographic details and CCDC numbers see the Supporting Information. (d) The DFT optimized geometry of Ad[10]CPP⁺ cation (at B3LYP-D3(BJ)/def2-SVP level). Color code: C yellow, N blue, O red and H white. Other hydrogen atoms, solvent molecules and counter ions are omitted for the sake of clarity.

Ad[10]CPP-OH with excess trifluoroacetic acid (TFA). The isolation of a solid Ad[10]CPP•BF₄ or Ad[10]CPP•TFA sample proved to be elusive despite extensive efforts, attributed to the intrinsic instability of the cationic macrocycle under neutral conditions. Specifically, the acridinium moiety is highly vulnerable to nucleophilic attack, readily reverting to Ad[10]CPP-OH upon exposure to moisture. A TFA titration experiment revealed that the interconversion between Ad[10]CPP⁺ and Ad[10]CPP-OH occurs within the TFA range between 1.0×10^{-4} to 1.0×10^{-5} M in CH₂Cl₂ (Figure S26). This highlights the dependency of the thermodynamic stability of the cationic macrocycle on acidic conditions. Strain energy calculations revealed a significant increase from 38.7 kcal/mol for Ad[10]CPP-OH to 56.2 kcal/mol for Ad[10]CPP⁺. This substantial increase in ring strain imposes a considerable thermodynamic penalty, thereby disfavoring the formation of the cationic species (Figure S73 and Table S5). Furthermore, the instability also hinders the crystal growth of the cationic macrocycle. Specifically, the gradual evaporation of the volatile acid (e.g., TFA), which is essential for maintaining the cationic state, prevented the growth of diffraction-quality crystals over time. Despite months of dedicated efforts, including crystallization attempts in a nitrogen-filled glovebox, we were unable to obtain a single crystal suitable for X-ray diffraction analysis. Consequently, we employed density functional theory (DFT) calculations at the B3LYP-D3(BJ)/def2-SVP level to

elucidate the structural characteristics of the acridinium macrocycle. The computational results depicted an elliptical nanoring with a long axis of 14.0 Å and a short axis of 13.6 Å. The acridinium aromatic plane is oriented at an angle of 61.0° relative to the macrocyclic plane (Figure 1d). The torsion angles between the acridinium unit and its adjacent phenylene moieties were measured to be 51.5° and 67.3°, respectively. These values are notably larger than those between other phenylene rings (22.1° to 36.5°), a difference attributed to the steric hindrance between the close-contacted hydrogen atoms on acridinium and adjacent phenylene units (Figure S76).

Photophysical properties

With the acridinium macrocycle in hand, we proceeded to investigate the photophysical properties of this compound together with its two precursor macrocycles (Figure 3a and Table S1). The absorption spectra of Ad[10]CPP-H and Ad[10]CPP-OH were nearly identical, both exhibiting overlapping absorption bands between 300 and 440 nm and lacking a broad charge-transfer band. Both compounds showed an absorption maximum (λ_{max}) at 326 nm, accompanied by a shoulder at approximately 378 nm. Time-dependent density functional theory (TD-DFT) calculations indicate that the major absorption at 326 nm arises from a combination of transitions: for Ad[10]CPP-H, these are HOMO-2 → LUMO, HOMO-1 → LUMO+1 and HOMO → LUMO+1 (Table S6); for Ad[10]CPP-OH,



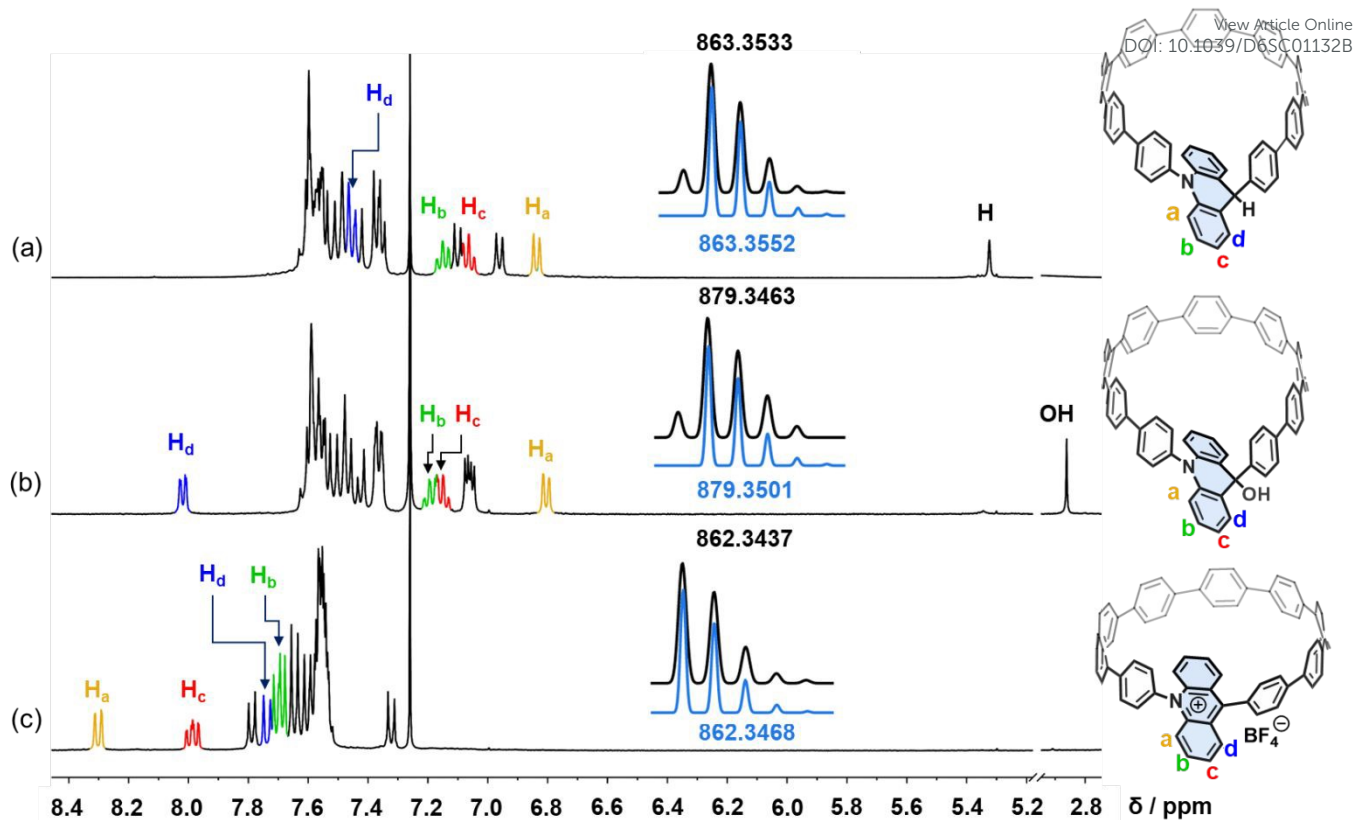


Figure 2. Partial ^1H NMR spectra (400 MHz, CDCl_3 , 298 K) of (a) **Ad[10]CPP-H**, (b) **Ad[10]CPP-OH**, and (c) **Ad[10]CPP-OH** upon addition of excess aqueous HBF_4 (40%). Insets show the experimental (black) and simulated (blue) MALDI-TOF-HRMS data for **Ad[10]CPP-H**, **Ad[10]CPP-OH**, and **Ad[10]CPP $^+$** .

they are HOMO-2 \rightarrow LUMO, and HOMO \rightarrow LUMO+1 (Table S7). In both **Ad[10]CPP-H** and **Ad[10]CPP-OH**, the HOMO is primarily confined to the oligoparaphenylene loop, indicating that the acridine segment acts as an electron donor in these neutral systems. A more pronounced spectroscopic change was observed upon protonating **Ad[10]CPP-OH** to form **Ad[10]CPP $^+$** . The absorption maximum λ_{max} of **Ad[10]CPP $^+$** was observed at 332 nm (Figure 3a), which is slightly blue-shifted compared to [10]CPP ($\lambda_{\text{max}} = 341 \text{ nm}$)^[66] but red-shifted relative to **Ad[10]CPP-OH** ($\lambda_{\text{max}} = 326 \text{ nm}$). The main absorption band of **Ad[10]CPP $^+$** is attributed to HOMO-1 \rightarrow LUMO+1 and HOMO \rightarrow LUMO+2 transitions (Table S8). Additionally, a shoulder peak appeared at around 365 nm, along with a broad characteristic charge-transfer band spanning from 420 nm to nearly 700 nm. TD-DFT calculations attribute this broad band to several transitions, including HOMO-4 \rightarrow LUMO, HOMO-2 \rightarrow LUMO, HOMO-1 \rightarrow LUMO, and HOMO \rightarrow LUMO. The frontier molecular orbital calculations further reveal that the HOMO of **Ad[10]CPP $^+$** is localized on the oligoparaphenylene loop, while the LUMO is confined to the acridinium unit and its adjacent aromatic rings (Figure 3b). This distinct spatial separation of orbitals is characteristic of a donor-acceptor system. Compared to **Ad[10]CPP-OH**, the HOMO and LUMO energy levels of **Ad[10]CPP $^+$** are lowered by approximately 2.11 eV and 0.2 eV (Figure 3b). This decrease in frontier molecular orbital energy is attributed to the formation of a rigid cationic framework and electron delocalization within the acridinium fragment, which

significantly stabilizes the entire π -system, particularly the HOMO.

The fluorescence properties of **Ad[10]CPP-H** and **Ad[10]CPP-OH** were found to be similar. Both exhibited emission bands at nearly identical wavelengths ($\lambda_{\text{em}} = 467 \text{ nm}$ for **Ad[10]CPP-H** and 466 nm for **Ad[10]CPP-OH**; Figure 3a) and high absolute fluorescence quantum yields ($\Phi_{\text{F}} = 70.9\%$ for **Ad[10]CPP-H** and 67.3% for **Ad[10]CPP-OH**; Figure S32, S33). Their singlet excited-state lifetimes (τ) were measured via time-resolved fluorescence spectroscopy as 2.48 ns for **Ad[10]CPP-H**, and 2.40 ns for **Ad[10]CPP-OH**, respectively (Figure S35, S36). A pronounced change was observed upon protonation of **Ad[10]CPP-OH**. The gradual addition of TFA to **Ad[10]CPP-OH** led to significant fluorescence quenching, with emission nearly completely suppressed upon full conversion to **Ad[10]CPP $^+$** (Figure S27). The cationic species **Ad[10]CPP $^+$** itself displayed very weak fluorescence with an emission maximum blue-shifted to 435 nm (Figure 3a). This weak emission further decreased in intensity and underwent an additional blue shift as the concentration of TFA was further elevated (Figure S28). The stability of **Ad[10]CPP $^+$** is contingent on excess acid, a condition that inevitably modifies its photophysical behavior, resulting in a pronounced acid concentration-dependent blue shift emission. This phenomenon likely arises because the acidic environment alters the excited-state decay pathway, potentially favoring radiative transition from a higher-energy



localized excited (LE) state on the acridinium moiety (Figure S30)

DPAd•BF₄ first undergoes a reversible one-electron reduction to a radical species, followed by an irreversible one-electron

DOI: 10.1039/D6SC01473R

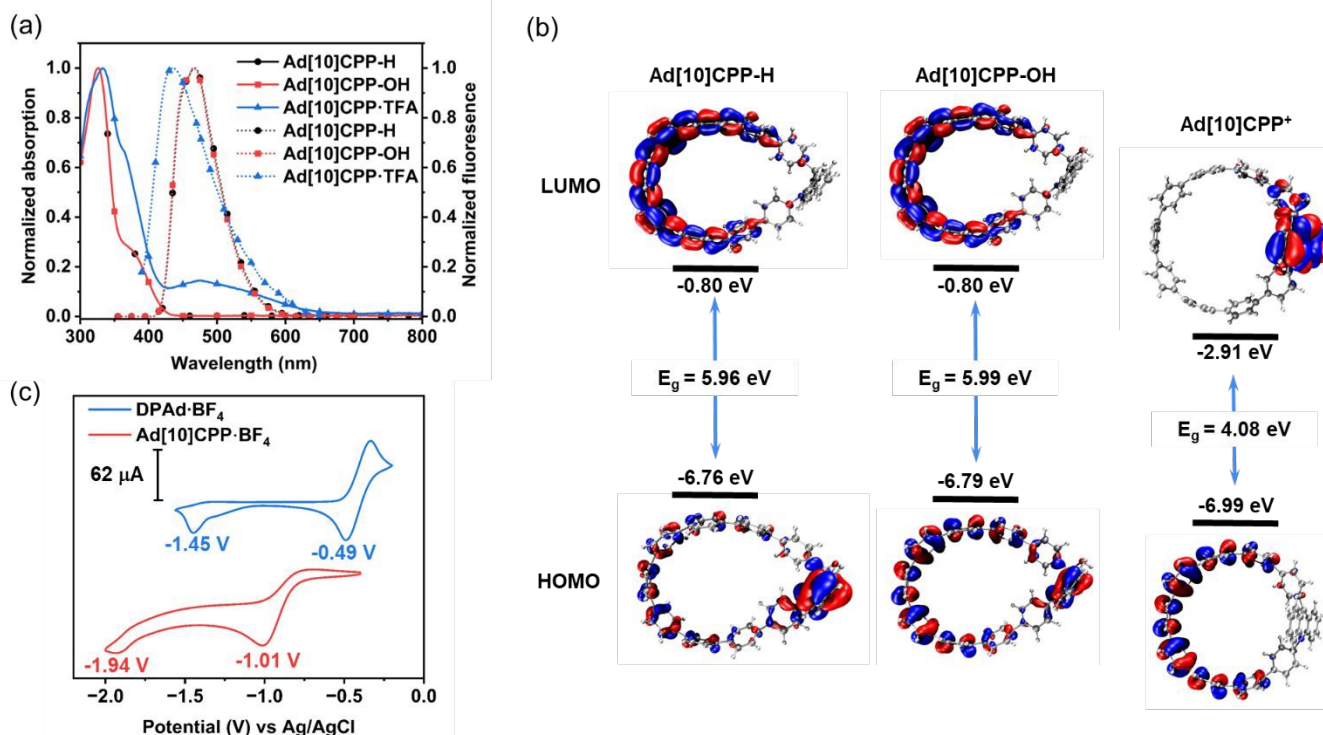


Figure 3. (a) UV-vis absorption (solid line) and fluorescence emission (dotted line) spectra of Ad[10]CPP-H ($\lambda_{\text{ex}} = 325$ nm) (black circle), Ad[10]CPP-OH ($\lambda_{\text{ex}} = 325$ nm) (red square), and Ad[10]CPP-TFA (blue triangle) measured in CH₂Cl₂ solutions (1×10^{-5} M) at room temperature. Ad[10]CPP-TFA sample is prepared by adding excess trifluoroacetic acid into Ad[10]CPP-OH, maintaining acid concentration at 1.0×10^{-3} M. (b) The DFT calculated frontier molecular orbitals and energy levels of Ad[10]CPP-H, Ad[10]CPP-OH and Ad[10]CPP•. (c) CV of 1.0 mM DPAAd•BF₄ in CH₂Cl₂ solution and Ad[10]CPP•BF₄ in CH₃CN solution (Ag/AgCl, 0.1 M n-Bu₄NBF₄, 100 mV/s).

The absolute fluorescence quantum yield of Ad[10]CPP• was determined to be only 0.95% (Figure S34) and the singlet excited-state lifetime was measured to be 1.88 ns (Figure S37). Based on these values, the nonradiative decay rate constant ($k_{\text{nr}} = 5.3 \times 10^8 \text{ s}^{-1}$) is significantly larger than the radiative decay rate constant ($k_{\text{r}} = 5.1 \times 10^6 \text{ s}^{-1}$), indicating that the excited-state energy of Ad[10]CPP• is primarily dissipated through non-radiative pathways. To gain further insight into the nature of the emissive state, we examined the emission spectra of Ad[10]CPP• in solvents of varying polarity (CCl₄, CHCl₃, C₂H₂Cl₄, CH₂Cl₂, and C₂H₄Cl₂). A small negative solvatochromic effect of approximately 20 nm was observed (Figure S29), suggesting that the emissive state is likely a LE state with only minor ICT character^[67, 68]. Several donor-acceptor cycloparaphenylene derivatives have been reported to exhibit low quantum yields due to significant spatial HOMO-LUMO separation that promotes non-radiative deactivation of the excited state^[34, 35, 69-77].

Electrochemical properties

The electrochemical behavior of Ad[10]CPP• was elucidated through cyclic voltammetry (CV) and differential pulse voltammetry (DPV), with DPAAd• serving as a comparative control (Figure 3c and Figure S41, S42). The reference compound DPAAd•BF₄ revealed two distinct reduction waves at -0.49 V and -1.45 V (vs Ag/AgCl), respectively^[78]. These waves correspond to two single-electron reduction processes, where

reduction to form an anionic intermediate, which then captures a proton to afford DPAd-H (Figure S38a)^[79-81]. Ad[10]CPP•BF₄ displays a similar two single-electron reduction processes with two notable distinctions. Firstly, the redox waves were shifted to a more negative potential by approximately 400 mV, appearing at -1.01 V and -1.94 V, respectively. Secondly, the transition to the radical state exhibited a semi-reversible nature (Figure S38b). The calculated radical state Ad[10]CPP• shows a geometry between the teardrop shape of Ad[10]CPP-H/Ad[10]CPP-OH and the close-to-circle shape of Ad[10]CPP•, namely, the ratio of long axis and short axis of the radical state falls between them (Figure S74). It is postulated that a geometrical change occurs upon the formation of the radical species, which, when attempting to revert the acridinium form, requires the molecular framework to overcome significant ring strain. In our subsequent efforts, we attempted to generate and characterize Ad[10]CPP•, the radical state of the macrocycle. As previously noted, the acridinium form Ad[10]CPP• is only stable in moderately acidic conditions, which posed a challenge for generating radicals through reduction with active metals or cobaltocene, as these reagents tend to react with the acid first. To circumvent this issue, we tried an alternative strategy involving the oxidation of Ad[10]CPP-H to achieve the radical state by treating Ad[10]CPP-H with nitrosonium tetrafluoroborate (NOBF₄), a well-known one-electron oxidizing agent. To our surprise, Ad[10]CPP-dimers were generated after quenching the solution with air, as indicated by the HR-MS



spectra (Figure S24). This result suggests that the generated radical species is highly prone to dimerization. We were able to isolate the dimers. The ^1H NMR and ^1H - ^1H COSY spectra (Figure S52 and S53) indicated a mixture of two compounds in a $\sim 7:3$ ratio with very similar structures, as they were not differentiated by diffusion constants in the DOSY spectrum (Figure S55) nor the analytical HPLC trace (Figure S56). This also explains the lack of hyperfine splitting pattern in the EPR spectrum (Figure S47a). Further oxidizing the isolated dimers produces a broad near-infrared absorption band in the UV-vis-NIR spectrum ranging from 1000 nm to 2000 nm, with λ_{max} at 1574 nm (Figure S58), possibly coming from diradical dication of the dimers^[82]. A plausible mechanism for the formation of **Ad[10]CPP-dimers** is illustrated in Figure S54. Oxidation of **Ad[10]CPP-H** generates a prochiral radical cation, which can dimerize by forming a new σ -bond at the *para* positions relative to the nitrogen atom. This process, accompanied by the loss of two protons, yields a *meso* dimer and a pair of racemic dimers. The inherent strain in **Ad[10]CPP-H** induces an electronic effect that governs a highly selective dimerization pathway, leading to the formation of giant double nano hoops.

Host and guest interactions

With the structure of **Ad[10]CPP⁺** well characterized, we proceeded to evaluate its host capabilities for binding guest molecules, focusing on C_{60} due to the expected similarity in cavity size between **Ad[10]CPP⁺** and [10]CPP^[45]. Significant chemical shift changes in the ^1H NMR spectra of **Ad[10]CPP•TFA** upon the addition of C_{60} provided clear evidence of strong supramolecular interactions between the two species (Figure

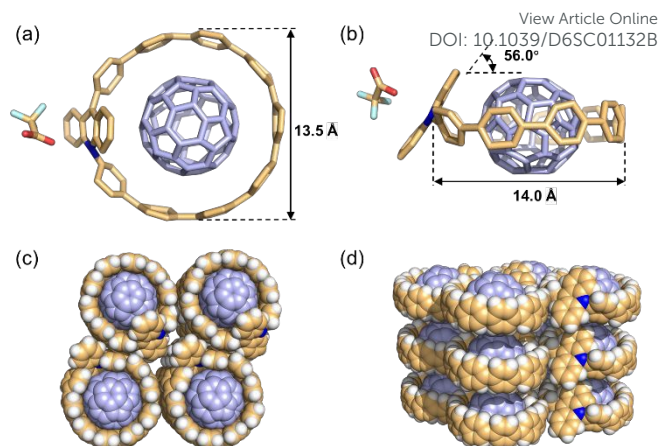


Figure 4. (a) Top view and (b) side view of the X-ray solid-state structure of $\text{C}_{60}\text{-Ad[10]CPP}\cdot\text{TFA}$. Hydrogen atoms are omitted for clarity. (c) Top view and (d) side view of crystal packing showing columnar stacks of $\text{C}_{60}\text{-Ad[10]CPP}\cdot\text{TFA}$, solvent molecules and counterions are omitted for clarity. Color code: C, tan/lavender; N, blue; O, red; F, pale cyan. For crystallographic details and CCDC numbers see the Supporting Information.

S60). The binding constant of **Ad[10]CPP•TFA** and C_{60} was determined to be $(2.18 \pm 0.27) \times 10^4 \text{ M}^{-1}$ (Figure S61) by NMR titration experiments, which are smaller than [10]CPP ($2.79 \pm 0.03) \times 10^6 \text{ M}^{-1}$ for C_{60} characterized by fluorescence-quenching experiments^[44].

After multiple attempts, we successfully obtained single crystals of the host-guest complex $\text{C}_{60}\text{-Ad[10]CPP}\cdot\text{TFA}$ suitable for X-ray diffraction analysis. The crystal structure unambiguously confirms a 1:1 host-guest complex, with C_{60} guest residing within the cavity of **Ad[10]CPP•TFA** (Figure 4). The

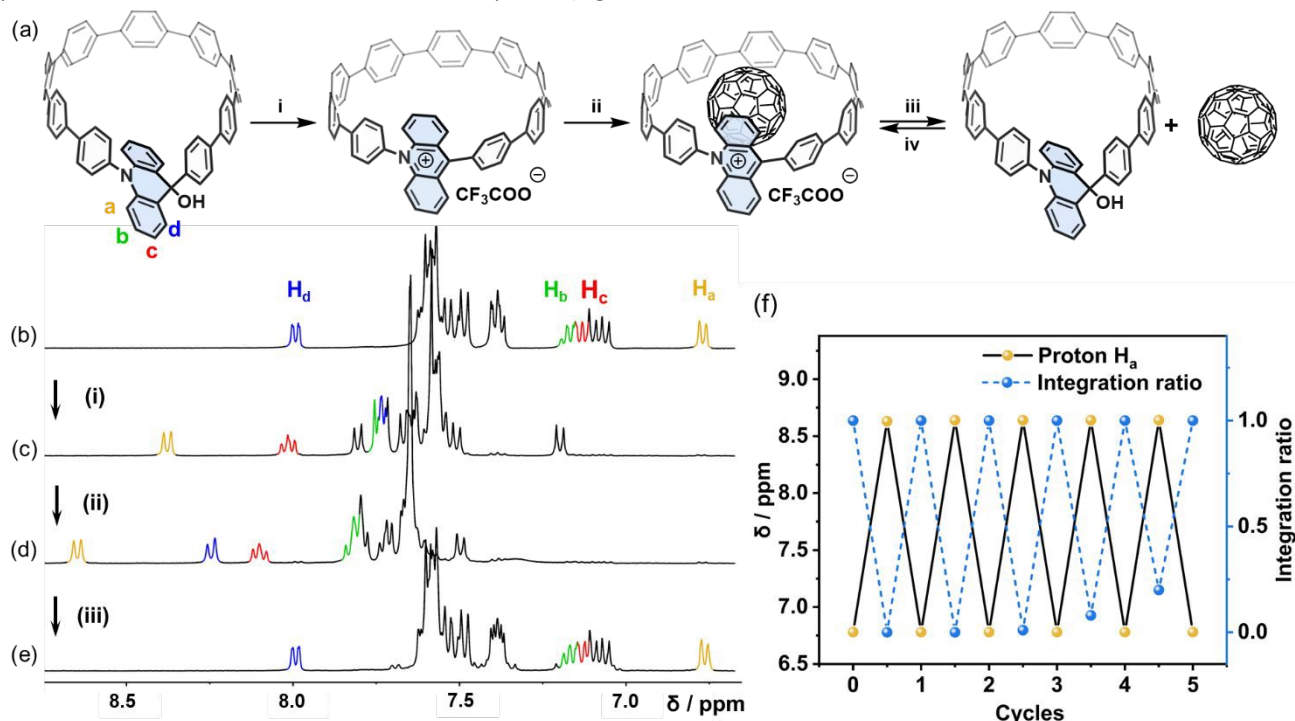


Figure 5. (a) Schematic representation of **acid-base** responsive capture and release of C_{60} ($0 \sim 4.09 \text{ mM}$) by macrocycle **Ad[10]CPP•TFA** (0.53 mM) in CD_2Cl_2 . Conditions and reagents: (i) TFA, CD_2Cl_2 , (ii) C_{60} , CD_2Cl_2 , ultrasound, (iii) TEA, CD_2Cl_2 , (iv) TFA, CD_2Cl_2 , ultrasound. ^1H NMR spectra (400MHz, CD_2Cl_2 , 298 K) of (b) **Ad[10]CPP•OH** and with sequential addition of (c) 5 eq of TFA, (d) 1.5 eq of C_{60} , (e) 5 eq of TEA. (f) Capture and release of C_{60} cycles of **Ad[10]CPP•TFA** under acid/neutral conditions, monitored by the ^1H NMR spectra.



cycloparaphenylene host exhibits a slightly elliptical shape, with a long and short axes of 14.0 Å and 13.6 Å, respectively (Figure 4a, b). Further structural analysis reveals a more compact supramolecular interactions compared to $C_{60} \subset [10]CPP$, as evidenced by the shorter average distance (3.21 Å) from the equatorial carbon atoms of C_{60} to the nearest phenylene plane of the host, relative to the 3.44 Å observed in the latter^[45] (Figure S71). The torsion angles between the acridinium and its adjacent phenylene moieties are 53.8° and 75.8°, respectively, markedly larger than those between other phenylene rings (8.3°~29.0°), which can be attributed to steric repulsion from the hydrogen atoms at the acridinium-phenylene junctions (Figure S72). Additionally, the acridinium fragment forms a dihedral angle of 57.2° with the macrocyclic plane (Figure 4b). Collectively, we propose that this strained, elliptical structure imposes a certain compression upon C_{60} encapsulation, which diminishes the optimal host-guest complementarity achieved in the nearly circular [10]CPP complex, thereby accounting for the lower binding constant.

In order to assess the stabilizing effect of C_{60} encapsulation on the $Ad[10]CPP^+$ host, we conducted systematic titration experiments using TFA. The protonation processes of $Ad[10]CPP-OH$ by TFA were monitored via characteristic NMR signals, both in the presence and absence of C_{60} (Figures S62 and S63). A change in solvent (CH_2Cl_2 to $C_2Cl_4D_2$) lowered the concentration of TFA required for the complete conversion of $Ad[10]CPP-OH$ to $Ad[10]CPP^+$. At a TFA concentration of 1.0×10^{-4} M, the conversion of free $Ad[10]CPP-OH$ was negligible, whereas partial conversion was achieved when C_{60} was present. This stabilization effect was further confirmed at a TFA concentration of 2.0×10^{-4} M, where $Ad[10]CPP-OH$ alone underwent incomplete conversion, but full conversion was achieved in the presence of excess C_{60} (Figures S64 and S65). These results demonstrate that host-guest complexation stabilizes the vulnerable structure of the host, thereby reducing the acid requirement for stabilizing the cationic host structure. This provides direct evidence that C_{60} substantially reinforces the molecular scaffold via π - π interactions. The encapsulation improves its stability against atmospheric moisture compared to the empty host, enabling the successful growth of single crystals suitable for X-ray diffraction, ultimately allowing us to resolve the structure of the $C_{60} \subset Ad[10]CPP \cdot TFA$ complex.

Stimulus responsive system

With the binding affinity between $Ad[10]CPP \cdot TFA$ and C_{60} measured and the structure of host-guest complex characterized, we then explored the acid-base stimuli responsive properties of the host-guest complex (Figure 5a). Gradually adding five equivalents of TFA to an NMR tube containing a CD_2Cl_2 solution of $Ad[10]CPP-OH$ (Figure 5b) caused a significant chemical shift change in the proton associated with the acridinium moiety. Specifically, H_a shifted from 6.78 ppm to 8.37 ppm, indicating complete transformation to $Ad[10]CPP \cdot TFA$ (Figure 5c). Subsequently, adding 1.5 equivalents of C_{60} to the same NMR tube caused H_a to shift further downfield to 8.64 ppm, attributed to the formation of

the host-guest complex $C_{60} \subset Ad[10]CPP \cdot TFA$ (Figure 5d). Adding five equivalents of triethylamine (TEA) to the solution caused the H_a signal to revert to 6.78 ppm, indicating the macrocycle had completely transformed back to $Ad[10]CPP-OH$ (Figure 5e). Since the cavity of $Ad[10]CPP-OH$ is not suitable for C_{60} (Figure S59), the guest molecule is then released to the solution. The acid-base switch process is reversible for at least 5 cycles, as monitored by 1H NMR spectroscopy (Figure 5f and Figure S67).

Conclusions

In summary, we successfully synthesized and characterized an acridinium-functionalized cycloparaphenylene derivative, $Ad[10]CPP^+$. Structural characterizations indicate that $Ad[10]CPP^+$ adopts a nearly circular configuration similar to [10]CPP, with increased torsion angles in the acridinium moiety due to steric hindrance. Electrochemical studies reveal two well-separated reduction peaks for $Ad[10]CPP^+$, suggesting its potential to form a radical species, $Ad[10]CPP^{\cdot}$. However, attempts to generate $Ad[10]CPP^{\cdot}$ through oxidation resulted in its dimerization, yielding giant double nanohoops. $Ad[10]CPP^+$ also demonstrates strong host-guest interactions with electron-rich fullerenes, as evidenced by NMR spectroscopy and single-crystal X-ray analysis. Furthermore, $Ad[10]CPP^+$ can undergo reversible structural transformations in response to chemical stimuli, enabling controlled capture and release of fullerene guest under alternating acidic and basic conditions for multiple cycles. The acid-base triggered guest capture and release of $Ad[10]CPP^+$ represents a valuable addition to the cycloparaphenylene family. Its key advantage lies in the highly confined cavity and switchable cationic character. Our current efforts are focusing on leveraging multi-acridinium motifs to develop advanced functional systems for applications on sensing wider guests.

Author contributions

C. C. conceived and supervised the project. J. Ming. performed most synthesis and characterization experiments. J. Z. and P. Y. conducted the calculations. Y. H., J. J., X. Z. and H. Z. helped with synthesis starting materials. K. L., D.Z., P. L. and J. Miao helped with characterizations. All authors contributed to manuscript writing.

Conflicts of interest

There are no conflicts to declare.

Data availability

Supporting Information is available and includes additional experimental details, materials and methods, 1H and ^{13}C NMR, ($^1H, ^1H$)-COSY NMR, MS, and UV-vis-IR spectra, EPR spectra, crystallographic data, and computational details (PDF). Deposition Numbers 2449559, 2449558 and 2449561 contain the supplementary crystallographic data for this paper. These



data can be obtained free of charge via the joint Cambridge Crystallographic Data Centre (CCDC) and Fachinformationszentrum Karlsruhe Access Structures service.

Acknowledgements

This work was supported by the Fundamental Research Funds for the Central Universities and NSFC 22171193. We thank Professor Lihua Yuan and Professor Xiaowei Li at Sichuan University for their help with UV-vis and fluorescence spectroscopy. We thank Yuxuan He, Professor Zhengyang Bin and Professor Jinsong You at Sichuan University for their help with the lifetimes of the singlet excited states and the fluorescence quantum yield; We thank Yimeng Hu, Professor Liangfang Zhu and Professor Changwei Hu at Sichuan University for UV-Vis-NIR spectroscopy. We thank Lingyan Sun, Professor Cheng Zhang at Sichuan University for their help with HPLC chromatogram. We thank Dr. Jing Li, Dr Chunxia Wang and Dr. Dongyan Deng from Sichuan University for HR-MS and NMR testing, respectively. We thank Dr Fucheng Leng at Westlake University for the single-crystal crystallography. Computational work was supported by the Center for Computational Science and Engineering and the CHEM High-Performance Supercomputer Cluster (CHEM-HPC) of the Department of Chemistry, Southern University of Science and Technology.

References

- R. Jasti, J. Bhattacharjee, J. B. Neaton, C. R. Bertozzi, Synthesis, Characterization, and Theory of [9]-, [12]-, and [18]Cycloparaphenylene: Carbon Nanohoop Structures. *J. Am. Chem. Soc.* **2008**, *130*, 17646-17647.
- S. E. Lewis, Cycloparaphenylenes and related nanohoops. *Chem. Soc. Rev.* **2015**, *44*, 2221-2304.
- Y. Segawa, A. Yagi, K. Matsui, K. Itami, Design and Synthesis of Carbon Nanotube Segments. *Angew. Chem. Int. Ed.* **2016**, *55*, 5136-5158.
- Y. Xu, M. von Delius, The Supramolecular Chemistry of Strained Carbon Nanohoops. *Angew. Chem. Int. Ed.* **2020**, *59*, 559-573.
- J. Wang, X. Zhang, H. Jia, S. Wang, P. Du, Large π -Extended and Curved Carbon Nanorings as Carbon Nanotube Segments. *Acc. Chem. Res.* **2021**, *54*, 4178-4190.
- Y. Li, H. Kono, T. Maekawa, Y. Segawa, A. Yagi, K. Itami, Chemical Synthesis of Carbon Nanorings and Nanobelts. *Acc. Mater. Res.* **2021**, *2*, 681-691.
- X. Li, S. Guo, H. Jiang, Recent advances in functionalized cycloparaphenylenes: from molecular design to applications. *Chem. Commun.* **2025**, *61*, 9836-9852.
- M. Hermann, D. Wassy, B. Esser, Conjugated Nanohoops Incorporating Donor, Acceptor, Hetero- or Polycyclic Aromatics. *Angew. Chem. Int. Ed.* **2021**, *60*, 15743-15766.
- E. Kayahara, R. Qu, S. Yamago, Bromination of Cycloparaphenylenes: Strain - Induced Site - Selective Bis - Addition and Its Application for Late - Stage Functionalization. *Angew. Chem. Int. Ed.* **2017**, *56*, 10428-10432.
- E. Kayahara, T. Hayashi, K. Takeuchi, F. Ozawa, K. Ashida, S. Ogoshi, S. Yamago, Strain - Induced Double Carbon - Carbon Bond Activations of Cycloparaphenylenes by a Platinum Complex: Application to the Synthesis of Cyclic Diketones. *Angew. Chem. Int. Ed.* **2018**, *57*, 11418-11421.
- T. Terabayashi, E. Kayahara, Y. Zhang, Y. Mizuhata, N. Tokitoh, T. Nishinaga, T. Kato, S. Yamago, Synthesis of Twisted [n]Cycloparaphenylene by Alkene Insertion. *Angew. Chem. Int. Ed.* **2023**, *62*, e202214960.
- J. M. Fehr, N. Myrthil, A. L. Garrison, T. W. Price, S. A. Lopez, R. Jasti, Experimental and theoretical elucidation of SPAAC kinetics for strained alkyne-containing cycloparaphenylenes. *Chem. Sci.* **2023**, *14*, 2839-2848.
- T. D. Clayton, J. M. Fehr, T. W. Price, L. N. Zakharov, R. Jasti, Pinwheel-like Curved Aromatics from the Cyclotrimerization of Strained Alkyne Cycloparaphenylenes. *J. Am. Chem. Soc.* **2024**, *146*, 30607-30614.
- K. Lan, C. Zhang, Y. Li, C. Hu, Z. Su, C. Cheng, Strain Energy Prompted Tunable Aggregation-Induced Emission Property of Tetraphenylethylene. *Angew. Chem. Int. Ed.* **2025**, *64*, e202507763.
- K. Lan, S. Zhang, Y. Lu, P. Yu, J. Chen, C. Cheng, Strain Energy Induced Rotary Speed Acceleration in a Light- Driven Molecular Motor. *Angew. Chem. Int. Ed.* **2025**, *64*, e202507487.
- Z. A. Huang, C. Chen, X. D. Yang, X. B. Fan, W. Zhou, C. H. Tung, L. Z. Wu, H. Cong, Synthesis of Oligoparaphenylene-Derived Nanohoops Employing an Anthracene Photodimerization-Cycloreversion Strategy. *J. Am. Chem. Soc.* **2016**, *138*, 11144-11147.
- Y. Segawa, M. Kuwayama, K. Itami, Synthesis and Structure of [9]Cycloparaphenylene Catenane: An All-Benzene Catenane Consisting of Small Rings. *Org. Lett.* **2020**, *22*, 1067-1070.
- K. Li, S. Yoshida, R. Yakushiji, X. Liu, C. Ge, Z. Xu, Y. Ni, X. Ma, J. Wu, S. Sato, Z. Sun, Molecular cylinders with donor-acceptor structure and swinging motion. *Chem. Sci.* **2024**, *15*, 18832-18839.
- G. Li, X. Wang, L. L. Mao, J. N. Gao, X. Shi, H. Li, Z. T. Li, Z. Y. Huo, Y. Chen, H. B. Yang, J. Chen, C. H. Tung, L. Z. Wu, H. Cong, Tubular All-Benzene Nanocarbon with Evolving Excited-State Chirality. *Angew. Chem. Int. Ed.* **2025**, e202518587
- W. Shi, Y. Hu, L. Leanza, Y. Shchukin, P. A. Hoffmann, M.-H. Li, C. Ning, Z.-Y. Cao, Y.-Q. Xu, P. Du, M. von Delius, G. M. Pavan, Y. Xu, Ring-in-Ring Assembly Facilitates the Synthesis of a [12]Cycloparaphenylene ABC-Type [3]Catenane. *Angew. Chem. Int. Ed.* **2025**, *64*, e202421459.
- L. Zhan, C. Dai, G. Zhang, J. Zhu, S. Zhang, H. Wang, Y. Zeng, C. H. Tung, L. Z. Wu, H. Cong, A Conjugated Figure-of-Eight Oligoparaphenylene Nanohoop with Adaptive Cavities Derived from Cyclooctatetrathiophene Core. *Angew. Chem. Int. Ed.* **2022**, *61*, e202113334.
- P. Fang, M. Chen, N. Yin, G. Zhuang, T. Chen, X. Zhang, P. Du, Regulating supramolecular interactions in dimeric macrocycles. *Chem. Sci.* **2023**, *14*, 5425-5430.
- A. A. Kamin, T. D. Clayton, C. E. Otteson, P. M. Gannon, S. Krajewski, W. Kaminsky, R. Jasti, D. J. Xiao, Synthesis and metalation of polycatechol nanohoops derived from fluorocycloparaphenylenes. *Chem. Sci.* **2023**, *14*, 9724-9732.
- M. S. Mirzaei, S. Mirzaei, V. M. Espinoza Castro, C. Lawrence, R. Hernández Sánchez, Dual molecular tweezers extending from a nanohoop. *Chem. Commun.* **2024**, *60*, 14236-14239.
- K. Kovida, J. Malinčík, C. M. Cruz, A. G. Campaña, T. Šolomek, Role of exciton delocalization in chiroptical properties of benzothiadiazole carbon nanohoops. *Chem. Sci.* **2025**, *16*, 1405-1410.
- Y. Hu, T. Li, T. Su, W. Shi, Y. Yu, B. Li, M.-H. Li, S. Zhang, Y.-Q. Xu, Q. Liu, D. Wu, Y. Xu, Crown ether-cycloparaphenylene hybrid multimacrocycles: insights into supramolecular gas sensing and biological potential. *Chem. Sci.* **2025**, *16*, 13115-13121.
- T. Kato, D. Imoto, A. Yagi, K. Itami, Making non-emissive [6]cycloparaphenylene fluorescent by simple multiple methyl substitution. *Chem. Sci.* **2025**, *16*, 18952-18958.



- 28 N. Liu, Y. Choi, Z. Zong, T. Feng, T. Kim, X.-S. Ke, BODIPY-Cycloparaphenylene Nanorings. *CCS Chem.* **2025**, *7*, 3650-3663.
- 29 M. Katsuma, S. Yasutomo, I. Kenichiro, Synthesis and Properties of Cycloparaphenylene-2,5-pyridylidene: A Nitrogen-Containing Carbon Nanoring. *Org. Lett.* **2012**, *14*, 1888-1891.
- 30 J. M. Van Raden, S. Louie, L. N. Zakharov, R. Jasti, 2,2'-Bipyridyl-Embedded Cycloparaphenylenes as a General Strategy To Investigate Nanohoop-Based Coordination Complexes. *J. Am. Chem. Soc.* **2017**, *139*, 2936-2939.
- 31 Y. Y. Fan, D. Chen, Z. A. Huang, J. Zhu, C. H. Tung, L. Z. Wu, H. Cong, An isolable catenane consisting of two Mobius conjugated nanohoops. *Nat. Commun.* **2018**, *9*, 3037.
- 32 J. H. May, J. M. Van Raden, R. L. Maust, L. N. Zakharov, R. Jasti, Active template strategy for the preparation of π -conjugated interlocked nanocarbons. *Nat. Chem.* **2023**, *15*, 170-176.
- 33 J. H. May, J. M. Fehr, J. C. Lorenz, L. N. Zakharov, R. Jasti, A High-Yielding Active Template Click Reaction (AT-CuAAC) for the Synthesis of Mechanically Interlocked Nanohoops. *Angew. Chem. Int. Ed.* **2024**, *63*, e202401823.
- 34 E. R. Darzi, E. S. Hirst, C. D. Weber, L. N. Zakharov, M. C. Lonergan, R. Jasti, Synthesis, Properties, and Design Principles of Donor-Acceptor Nanohoops. *ACS. Cent. Sci.* **2015**, *1*, 335-342.
- 35 J. M. Van Raden, E. R. Darzi, L. N. Zakharov, R. Jasti, Synthesis and characterization of a highly strained donor-acceptor nanohoop. *Org. Biomol. Chem.* **2016**, *14*, 5721-5727.
- 36 T. Drennhaus, D. Imoto, E. S. Horst, L. Lezius, H. Shudo, T. Kato, K. Bergander, C. G. Daniliuc, D. Leifert, A. Yagi, A. Studer, K. Itami, Cycloparaazine, a full-azine carbon nanoring. *Nat. Commun.* **2025**, *16*, 4643.
- 37 T. Wu, J. Yang, Y. Liu, C. Wang, J. Zhang, R.-H. Zheng, H. Yu, R. Liu, D. Lu, Size-controlled synthesis of N-doped [10]CPPs and investigation on the variations of their binding affinities with fullerene. *Chin. Chem. Lett.* **2025**, 112199.
- 38 S. Qiu, Y. Zhao, L. Zhang, Y. Ni, Y. Wu, H. Cong, D.-H. Qu, W. Jiang, J. Wu, H. Tian, Z. Wang, Axially N-Embedded Quasi-Carbon Nanohoops with Multioxidation States. *CCS Chem.* **2023**, *5*, 1763-1772.
- 39 X. Zhang, J. Jiang, K. Lan, D. Zhang, C. Cheng, Cycloparaphenylene-Type Hoops with Adaptive Cavities Derived from N,N'-diphenyldihydrodibenzo[a,c]phenazine. *Org. Lett.* **2025**, *27*, 10484-10488.
- 40 R. Frydrych, K. Senthilkumar, K. Ślusarek, M. Waliczek, W. Bury, P. J. Chmielewski, J. Cybińska, M. Stępień, Viologen-cycloparaphenylene hybrids: luminescent molecular nanocarbons for anion binding and specific vapor sorption. *Org. Chem. Front.* **2025**, *12*, 437-447.
- 41 S. Qiu, L. Zhang, D.-H. Qu, Z. Wang, Supercycloalkanes: dihydropyrazine-embedded macrocycles with flexible conformations resembling cycloalkanes. *Chem. Sci.* **2025**, *16*, 20464-20472.
- 42 L. Zhang, S. Qiu, S. Hu, H. Xu, X. Sun, W. Jiang, D.-H. Qu, Z. Wang, Cocrystals of axially N-embedded quasi-carbon nanohoops via modulating the electron affinity of guest acceptors. *Sci. China. Chem.* **2025**, *68*, 3154-3161.
- 43 D. Zhang, J. Liu, J. Ming, K. Lan, J. Jiang, H. Zhong, X. Zhang, Z. Bin, C. Cheng, Incorporating a Pyridinium into a Cycloparaphenylene: A Cati-ionic Donor-Acceptor Nanohoop with Reversible Redox Properties. *Sci. China. Chem.* **2026**, in press, doi:10.1007/s11426-11025-13313-11429.
- 44 T. Iwamoto, Y. Watanabe, T. Sadahiro, T. Haino, S. Yamago, Size-Selective Encapsulation of C₆₀ by [10]Cycloparaphenylene: Formation of the Shortest Fullerene-Peapod. *Angew. Chem. Int. Ed.* **2011**, *50*, 8342-8344.
- 45 J. Xia, J. W. Bacon, R. Jasti, Gram-scale synthesis and crystal structures of [8]- and [10]CPP, and the solid-state structure of C₆₀@[10]CPP. *Chem. Sci.* **2012**, *3*, 3018-3021.
- 46 T. Iwamoto, Y. Watanabe, H. Takaya, T. Haino, N. Yasuda, S. Yamago, Size- and Orientation- Selective Encapsulation of C₇₀ by Cycloparaphenylenes. *Chem. Eur. J.* **2013**, *19*, 14061-14068.
- 47 A. Stergiou, J. Rio, J. H. Griwatz, D. Arcon, H. A. Wegner, C. P. Ewels, N. Tagmatarchis, A Long-Lived Azafullerenyl Radical Stabilized by Supramolecular Shielding with a [10]Cycloparaphenylene. *Angew. Chem. Int. Ed.* **2019**, *58*, 17745-17750.
- 48 S. Wang, X. Li, X. Zhang, P. Huang, P. Fang, J. Wang, S. Yang, K. Wu, P. Du, A supramolecular polymeric heterojunction composed of an all-carbon conjugated polymer and fullerenes. *Chem. Sci.* **2021**, *12*, 10506-10513.
- 49 E. Ubasart, O. Borodin, C. Fuertes-Espinosa, Y. Xu, C. García-Simón, L. Gómez, J. Juanhuix, F. Gándara, I. Imaz, D. Maspoch, M. von Delius, X. Ribas, A three-shell supramolecular complex enables the symmetry-mismatched chemo- and regioselective bis-functionalization of C₆₀. *Nat. Chem.* **2021**, *13*, 420-427.
- 50 Y. Xu, F. Steudel, M. Y. Leung, B. Xia, M. von Delius, V. W. W. Yam, [n]Cycloparaphenylene- Pillar[5]arene Bismacrocycles: Their Circularly Polarized Luminescence and Multiple Guest Recognition Properties. *Angew. Chem. Int. Ed.* **2023**, *62*, e202302978.
- 51 P. J. Evans, L. N. Zakharov, R. Jasti, Synthesis of carbon nanohoops containing thermally stable cis azobenzene. *J. Photochem. Photobiol. A Chem.* **2019**, *382*, 111878.
- 52 X. Li, L. Jia, W. Wang, Y. Wang, D. Sun, H. Jiang, A nonalternant azulene-embedded carbon nanohoop featuring anti-Kasha emission and tunable properties upon pH stimuli-responsiveness. *J. Mater. Chem. C.* **2023**, *11*, 1429-1434.
- 53 T. Ide, W.-C. Huang, M. Horie, Tris-Azo Triangular Paraphenylenes: Synthesis and Reversible Interconversion into Radial π -Conjugated Macrocycles. *J. Am. Chem. Soc.* **2024**, *146*, 10246-10250.
- 54 S. Wu, J. Jie, L. Liu, L. Liu, S. Guo, X. Li, J. He, Z. Lian, Y. Wang, X. Xu, H. Su, X. Chen, H. Jiang, A Redox-Active π -Extended Tetrathiafulvalene-Based Carbon Nanohoop Featuring Unique Kasha/Anti-Kasha Dual Emissions: Structure, Photophysical Properties, and Photoconductivity. *Angew. Chem. Int. Ed.* **2025**, *64*, e202512167.
- 55 K. Kurihara, K. Yazaki, M. Akita, M. Yoshizawa, A Switchable Open/closed Polyaromatic Macrocycle that Shows Reversible Binding of Long Hydrophilic Molecules. *Angew. Chem. Int. Ed.* **2017**, *56*, 11360-11364.
- 56 J. Hu, J. S. Ward, A. Chaumont, K. Rissanen, J. M. Vincent, V. Heitz, H. P. Jacquot de Rouville, A Bis-Acrinium Macrocycle as Multi-Responsive Receptor and Selective Phase-Transfer Agent of Perylene. *Angew. Chem. Int. Ed.* **2020**, *59*, 23206-23212.
- 57 I. A. MacKenzie, L. Wang, N. P. R. Onuska, O. F. Williams, K. Begam, A. M. Moran, B. D. Dunietz, D. A. Nicewicz, Discovery and characterization of an acridine radical photoreductant. *Nature.* **2020**, *580*, 76-80.
- 58 H. P. Jacquot de Rouville, J. Hu, V. Heitz, N-Substituted Acrinium as a Multi-Responsive Recognition Unit in Supramolecular Chemistry. *ChemPlusChem* **2021**, *86*, 110-129.
- 59 H.-P. Jacquot de Rouville, C. Gourlaouen, D. Bardelang, N. Le Breton, J. S. Ward, L. Ruhlmann, J.-M. Vincent, D. Jardel, K. Rissanen, J.-L. Clément, S. Choua, V. Heitz, Viridium: A Stable Radical and Its π -Dimerization. *J. Am. Chem. Soc.* **2024**, *147*, 1823-1830.
- 60 S. Claude, J.-M. Lehn, F. Schmidt, J.-P. Vigneron, Binding of Nucleosides, Nucleotides and Anionic Planar Substrates by



- Bis-Intercalated Receptor Molecules. *J. Chem. Soc., Chem. Commun.* **1991**, 1182-1185.
- 61 H. Kawai, T. Takeda, K. Fujiwara, M. Wakeshima, Y. Hinatsu, T. Suzuki, Ultralong Carbon – Carbon Bonds in Dispirobis(10 - methylacridan) Derivatives with an Acenaphthene, Pyracene, or Dihydropyrycene Skeleton. *Chem. Eur. J.* **2008**, *14*, 5780-5793.
- 62 A. Petitjean, R. G. Khoury, N. Kyritsakas, J.-M. Lehn, Dynamic Devices. Shape Switching and Substrate Binding in Ion-Controlled Nanomechanical Molecular Tweezers. *J. Am. Chem. Soc.* **2004**, *126*.
- 63 W. Abraham, K. Buck, M. Orda-Zgadzaj, S. Schmidt-Schäffer, U.-W. Grummt, Novel photoswitchable rotaxanes. *Chem. Commun.* **2007**, 3094-3096.
- 64 X. Zhang, K. Lan, C. Cheng, Figure-Eight Bismacrocycles Derived from a Tetraphenylmethane Core and Oligoparaphenylene Loops. *Org. Lett.* **2024**, *26*, 7853-7857.
- 65 V. K. Patel, E. Kayahara, S. Yamago, Practical Synthesis of [n]Cycloparaphenylenes (n=5, 7-12) by H₂SnCl₄-Mediated Aromatization of 1,4-Dihydroxycyclo-2,5-diene Precursors. *Chem. Eur. J.* **2015**, *21*, 5742-5749.
- 66 T. Iwamoto, Y. Watanabe, Y. Sakamoto, T. Suzuki, S. Yamago, Selective and Random Syntheses of [n]Cycloparaphenylenes (n = 8-13) and Size Dependence of Their Electronic Properties. *J. Am. Chem. Soc.* **2011**, *133*, 8354-8361.
- 67 B. Carlotti, A. Cesaretti, C. G. Fortuna, A. Spalletti, F. Elisei, Experimental evidence of dual emission in a negatively solvatochromic push-pull pyridinium derivative. *Phys. Chem. Chem. Phys.* **2015**, *17*, 1877-1882.
- 68 P. Sumsalee, P. Morgante, G. Pieters, J. Crassous, J. Autschbach, L. Favereau, Negative solvatochromism and sign inversion of circularly polarized luminescence in chiral exciplexes as a function of solvent polarity. *J. Mater. Chem. C.* **2023**, *11*, 8514-8523.
- 69 T. Kuwabara, J. Orii, Y. Segawa, K. Itami, Curved Oligophenylenes as Donors in Shape-Persistent Donor-Acceptor Macrocycles with Solvatofluorochromic Properties. *Angew. Chem. Int. Ed.* **2015**, *54*, 9646-9649.
- 70 T. C. Lovell, Z. R. Garrison, R. Jasti, Synthesis, Characterization, and Computational Investigation of Bright Orange - Emitting Benzothiadiazole [10]Cycloparaphenylene. *Angew. Chem. Int. Ed.* **2020**, *59*, 14363-14367.
- 71 D. Chen, Y. Wada, Y. Kusakabe, L. Sun, E. Kayahara, K. Suzuki, H. Tanaka, S. Yamago, H. Kaji, E. Zysman-Colman, A Donor-Acceptor 10-Cycloparaphenylene and Its Use as an Emitter in an Organic Light-Emitting Diode. *Org. Lett.* **2023**, *25*, 998-1002.
- 72 V. Bliksted Roug Pedersen, T. W. Price, N. Kofod, L. N. Zakharov, B. W. Laursen, R. Jasti, M. Brøndsted Nielsen, Synthesis and Properties of Fluorenone-Containing Cycloparaphenylenes and Their Late-Stage Transformation. *Chem. Eur. J.* **2023**, *30*, e202303490.
- 73 P. Fang, Z. Cheng, W. Peng, J. Xu, X. Zhang, F. Zhang, G. Zhuang, P. Du, A Strained Donor-Acceptor Carbon Nano-hoop: Synthesis, Photophysical and Charge Transport Properties. *Angew. Chem. Int. Ed.* **2024**, *63*, e202407078
- 74 C. Brouillac, E. Dureau, O. Jeannin, J. Rault-Berthelot, C. Poriel, C. Quinton, Donor-Acceptor Nano-hoops: Impact of the Ratio and Arrangement of the Fluorenone and Carbazole Moieties. *J. Am. Chem. Soc.* **2025**, *147*, 11267-11276.
- 75 S. Guo, L. Liu, L. Liu, Y. Fan, H. Yang, J. He, Y. Wang, Z. Bo, X. Xu, X. Chen, H. Jiang, Naphthalene Diimide-Embedded Donor-Acceptor Carbon Nano-hoops: Photophysical, Photoconductive, and Charge Transport Properties. *ACS Appl. Mater. Interfaces.* **2025**, *17*, 5202-5212.
- 76 X. Li, L. Liu, L. Jia, Z. Lian, J. He, S. Guo, Y. Wang, X. Chen, H. Jiang, Acceptor engineering of quinone-based cycloparaphenylenes via post-synthesis for achieving white-light emission in single-molecule. *Nat. Commun.* **2025**, *16*, 467. [DOI: 10.1039/D6SC01132B](https://doi.org/10.1039/D6SC01132B)
- 77 T. C. Lovell, K. G. Fossnacht, C. E. Colwell, R. Jasti, Effect of curvature and placement of donor and acceptor units in cycloparaphenylenes: a computational study. *Chem. Sci.* **2020**, *11*, 12029-12035.
- 78 T. P. Vaid, A. K. Lytton-Jean, B. C. Barnes, Investigations of the 9,10-Diphenylacridyl Radical as an Isostructural Dopant for the Molecular Semiconductor 9,10-Diphenylanthracene. *Chem. Mater.* **2003**, *15*, 4292-4299.
- 79 P. Hapiot, J. Moiroux, J.-M. Savéant, Electrochemistry of NADH/NAD⁺ Analogues. A Detailed Mechanistic Kinetic and Thermodynamic Analysis of the 10-Methylacridan/10-Methylacridinium Couple in Acetonitrile. *J. Am. Chem. Soc.* **1990**, *112*, 1337-1343.
- 80 D. T. Hogan, T. C. Sutherland, Modern Spin on the Electrochemical Persistence of Heteroatom-Bridged Triphenylmethyl-Type Radicals. *J. Phys. Chem. Lett.* **2018**, *9*, 2825-2829.
- 81 S. A. Jonker, F. Ariese, J. W. Verhoeven, Cation complexation with functionalized 9 - arylacridinium ions: Possible applications in the development of cation - selective optical probes. *Red. Trav. Chim. Pays-Bas* **1989**, *108*, 109-115.
- 82 K. Kamada, S.-i. Fuku-en, S. Minamide, K. Ohta, R. Kishi, M. Nakano, H. Matsuzaki, H. Okamoto, H. Higashikawa, K. Inoue, S. Kojima, Y. Yamamoto, Impact of Diradical Character on Two-Photon Absorption: Bis(acridine) Dimers Synthesized from an Allenic Precursor. *J. Am. Chem. Soc.* **2012**, *135*, 232-241.



Supporting Information is available and includes additional experimental details, materials and methods, ^1H and ^{13}C NMR, ($^1\text{H},^1\text{H}$)-COSY NMR, MS, and UV-vis-IR spectra, EPR spectra, crystallographic data, and computational details (PDF). Deposition Numbers 2449559, 2449558 and 2449561 contain the supplementary crystallographic data for this paper. These data can be obtained free of charge via the joint Cambridge Crystallographic Data Centre (CCDC) and Fachinformationszentrum Karlsruhe Access Structures service.

[View Article Online](#)

DOI: 10.1039/D6SC01132B

